



## Calhoun: The NPS Institutional Archive

---

Faculty and Researcher Publications

Faculty and Researcher Publications Collection

---

1977-09

Giant resonances and bound collective states observed in the scattering of 92.5-MeV electrons from the closed-neutro-shell nucleus (89)Y between excitation energies from 2.0 to 55 MeV

Pitthan, R.



Calhoun is a project of the Dudley Knox Library at NPS, furthering the precepts and goals of open government and government transparency. All information contained herein has been approved for release by the NPS Public Affairs Officer.

**Dudley Knox Library / Naval Postgraduate School  
411 Dyer Road / 1 University Circle  
Monterey, California USA 93943**

<http://www.nps.edu/library>

## Giant resonances and bound collective states observed in the scattering of 92.5-MeV electrons from the closed-neutron-shell nucleus $^{89}\text{Y}$ between excitation energies from 2.0 to 55 MeV<sup>†</sup>

R. Pitthan, F. R. Buskirk, E. B. Dally,\* J. O. Shannon, and W. H. Smith

Department of Physics and Chemistry, Naval Postgraduate School, Monterey, California 93940

(Received 7 April 1977)

92.5-MeV electrons were used to study in  $^{89}\text{Y}$  the excitation range between 2 and 55 MeV. Above neutron threshold, broad electric resonances have been seen at 14.0 ( $63A^{-1/3}$ ) MeV ( $E2$ ,  $\Delta T = 0$ ) and 28 ( $125A^{-1/3}$ ) MeV ( $E2$ ,  $\Delta T = 1$ ). The total width of the isoscalar  $E2$  resonance is  $(4.5 \pm 0.4)$  MeV and its strength  $(56 \pm 6)\%$  energy-weighted sum rule ( $E2$ ,  $\Delta T = 0$ ). For the isovector  $E2$  resonance only a minimal value of 7 MeV for the width can be given which is connected with  $(48 \pm 5)\%$  of the isovector sum rule. The strength of the  $E1$  resonance [ $T_1$ ,  $(104 \pm 10)\%$  of the Thomas-Reiche-Kuhn sum rule] agrees well with  $(\gamma, n)$  measurements, thus giving a check for the accuracy of the evaluating methods employed. A structure around 19–20 MeV, believed to be the  $T_2$  part of the giant dipole resonance, carries  $(8 \pm 3)\%$  of the  $E1$  sum rule. In addition to these generally well known states, clustering of  $E3$  strength,  $(13 \pm 2)\%$  energy-weighted sum rule ( $E3$ ,  $\Delta T = 0$ ), was found at 6.75 and 8.05 MeV; the enveloping line shape of these clusters was best described by a Breit-Wigner term. Other concentrations of strength include  $E3$  at 2.6 MeV,  $(15 \pm 3)\%$  energy-weighted sum rule ( $E3$ ,  $\Delta T = 0$ ),  $E2$  at 4.0 MeV,  $(11 \pm 3)\%$  energy-weighted sum rule ( $E2$ ,  $\Delta T = 0$ ), and  $E3$  strength at 13.5 MeV. No resonance other than the  $E1$  was found around 17 MeV, thus ruling out in  $^{89}\text{Y}$  the existence of a monopole state with 100% sum rule proposed for  $^{90}\text{Zr}$  from  $(\alpha, \alpha')$  and  $(e, e')$  measurements. In contrast to heavy nuclei, no resonant  $3\hbar\omega$   $E3$  strength could be located.

NUCLEAR REACTIONS  $^{89}\text{Y}(e, e')$ ,  $E_0 = 92.5$  MeV. Measured  $d^2\sigma/d\Omega dE_x$ , bound and continuum states. Deduced multipolarity  $\lambda$ , reduced matrix element  $B(E\lambda)$ , radiative width  $\Gamma_r^0$ , sum rule exhaustion, single particle strength, and total width of the continuum and clustered states.

### I. INTRODUCTION

Nuclei with closed shells have played an important role in the discovery of giant resonances other than the dipole resonance.<sup>1</sup> The (isoscalar)  $E2$  state, for example, was found to be of identical width in the  $N = 82$  nuclei  $^{139}\text{La}$ ,  $^{140}\text{Ce}$ , and  $^{141}\text{Pr}$  before even the multipolarity or other properties were established with certainty.<sup>2</sup> The importance of the closed shell nuclei rests mainly with the fact that the continuum states have relatively small width, typically of the order of 3 MeV, and can therefore be recognized as resonant structures above the radiative ( $e, e'$ ) or nuclear ( $p, p'$ ) background.

A comparison between nuclei in the  $^{208}\text{Pb}$  ( $N = 126$ ,  $Z = 82$ )<sup>3</sup> and the  $^{140}\text{Ce}$  ( $N = 82$ ) region,<sup>4</sup> and the  $^{90}\text{Zr}$  ( $N = 50$ ) region<sup>5</sup> shows one fundamental difference. The ratio  $R$  of the width of the giant quadrupole resonance (GQR),  $\Gamma_{E2}$ , to the width of the giant dipole resonance (GDR)  $\Gamma_{E1}$  in the heavier nuclei is 0.65 to 0.75, but found to be 1.1 to 1.2 in  $^{90}\text{Zr}$ . Since  $^{90}\text{Zr}$  is the only nucleus for which  $R > 1$  has been reported, we thought it important to investigate the  $N = 50$  nucleus  $^{89}\text{Y}$ . It is reasonable to expect, and in fact borne out by the experiments carried out so far, nearly identical gross proper-

ties of the giant resonances in neighboring spherical nuclei.

Besides the question of the width of the otherwise well known  $E2$  ( $\Delta T = 0$ ) state (see, e.g., Ref. 6) there is the much less well known isovector ( $\Delta T = 1$ ) giant quadrupole resonance.<sup>7</sup> The latter is important for testing microscopic theories of collective excitations, but not too much is known over a wide variety of nuclei. Because it lies high in excitation energy, it easily exhausts the appropriate energy-weighted sum rule. The great width of these states, typically 7 MeV, makes the experiments the more difficult. Experiments require very good statistics and reliable knowledge of general and radiative background. Since much of our effort in the last two years went into improving just this knowledge we felt confident to be able to make more definitive statements about the strength and location of the  $E2$  ( $\Delta T = 1$ ) state in medium heavy nuclei than have been possible in the past.

Other unsolved problems in  $N = 50$  nuclei include the magnetic states, a proposed monopole state at 17 MeV,<sup>8,9</sup> exactly under the giant dipole resonance, and higher multipoles. The range of momentum transfer  $q$  was chosen not only to include the maxima of the  $E2$  and  $E3$  form factors but also to

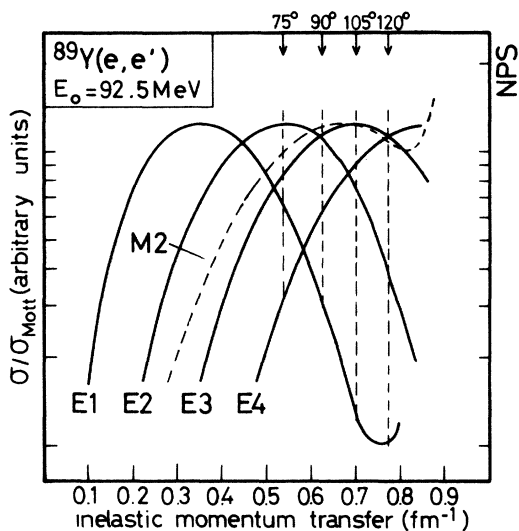


FIG. 1. DWBA cross sections for E1 to E4 and M2 transitions divided by the Mott cross section. The curves were normalized so that the first maxima are equal. The program of Tuan *et al.* (Ref. 25) was used with a transition charge density  $\rho_{tr}(r) = N_\lambda r^\lambda d\rho_0(r)/dr$  for the electric transitions and a transition current density  $j_{tr}(r) = N_\lambda d\rho_0(r)/dr$ . The figure shows that the momentum transfer covered by this experiment is selective for multipolarities 1 to 4.

allow the analysis of E1 and E4 transitions. Figure 1 shows arbitrarily normalized cross sections for various multipolarities. They were calculated with a distorted-wave Born approximation (DWBA) program using transition charge and current distributions peaking at the nuclear surface (Tassie model, see below). It is evident from Fig. 1 that a distinction between, e.g., M2 and E3 from the momentum transfer dependence alone is not easily possible. Since we, however, have restricted our measurements to forward angles, magnetic states other than M1 would have to exhaust several times the sum rule strength to show up noticeably.

## II. EXPERIMENTAL DETAILS

Electron scattering spectra were obtained at the Naval Postgraduate School (NPS) linear accelerator laboratory. Self-supporting targets with thicknesses between 110 and 180 mg/cm<sup>2</sup> were used. The scattering angles were 75°, 90°, 105°, and 120° at a constant elastic energy of 92.5 MeV. The corresponding momentum transfer  $q$  ranged from 0.54 to 0.76 fm<sup>-1</sup> for an excitation energy of 10 MeV.

The 120-MeV NPS linac consists of three S-band sections, driven by separate 20-MW klystrons. The repetition rate is 60 or 120 sec<sup>-1</sup>, depending on energy, and the duty cycle is about 0.0001.

Maximum average current at a resolution of 300 keV is 2  $\mu$ A. The deflection system consists of two 30° sector magnets and two quadrupole doublets, in an achromatic system designed by Brown.<sup>10</sup> The 40-cm spectrometer is 120°, and double focusing. All power supplies are regulated to better than one part in 10<sup>4</sup>. The beam spot on the target is less than 1 mm in diameter and extremely stable and reproducible.

The spectrometer does not have an open back and produces, therefore, an appreciable ghost peak. This peak is superimposed on any inelastic scattering spectrum, at a point where the magnetic field is low enough so that the numerous elastically scattered electrons hit the inside of the spectrometer chamber and scatter indirectly into the counters. In our spectrometer the ghost peak appears at an energy of 92% of that of the elastic peak, is known through measurements in <sup>12</sup>C, and can thus be accounted for in the evaluation, although this introduces an additional uncertainty for the cross sections in the 7- to 8-MeV region at forward angles.

The scattered electrons are finally detected in a 10 counter ladder in the focal plane of the spectrometer. The detector system consists of the 10 front counters and two backing counters arranged in 10 triple coincidence channels. The beam is limited to a value such that the accidental coincidence rate is always lower than 5%.

Due to the location of the accelerator, the target chamber is close to the deflection area. The difficulties associated with a relatively high background have been overcome by a very good overall beam stability backed by a system which only accepts counts if the beam intensity is within 10% of a preset value.

Also the beam monitor deserves comment. Usually a Faraday cup is employed, which produces high background if located near the target or extra focusing if far away. The NPS linac employs a five foil sealed secondary emission monitor located near the target. The background produced is low, it intercepts all the beam, and frequent comparison with a Faraday cup, which is removed during experiment, showed that the efficiency is stable to one part in 10<sup>4</sup>.

## III. EVALUATION

### A. Principles

The inelastic scattering spectra were measured relative to the elastic cross sections. The latter were evaluated using the phase-shift code of Fischer and Rawitscher.<sup>11</sup> Although this is a relatively old program, comparison with a more recent one<sup>12</sup> showed that the results are in agreement of better

than 0.5% with the latter. The charge distribution parameters  $c = 4.86$  fm and  $t = 2.38$  fm were taken from the work of Fivozinsky *et al.*<sup>13</sup> Schwinger and bremsstrahlung corrections<sup>14</sup> were performed on the elastic cross sections.

Three different kinds of background contribute to the observed inelastic spectra. The first is the general room background measured with "target-out," which in our case is small due to the directional coincidence applied in the counting system and very constant over time, i.e., independent of the tuning of the machine. The second is the "target-in" background which consists mainly of electrons which are originally scattered by the target but which penetrate the counter shielding or undergo subsequent scattering in the walls of the spectrometer. The third type of background is the elastic radiation tail which is caused by photon emission before, during, and after scattering and additional energy straggling and ionization. While conventional wisdom knows that the radiation tail (RT) cannot be calculated exactly enough in heavy nuclei, our results show that in fact it can. The progress made in this direction is described elsewhere<sup>15</sup>; here we only want to note that we are able to describe our total background (BGR) as a function of energy  $E_f$  of the outgoing electron between 5- and 40-MeV excitation energy by the formula:

$$\text{BGR}(E_f) = P_1 + P_2 \times \frac{1}{E_f} + P_3 \times \text{RT}.$$

This expression for BGR is incorporated in a line shape fitting routine with the  $P_i$  being fitted parameters. While  $P_1$  is close to the value expected from the accidental coincidence rate,  $P_2$  turns out to be small and  $P_3$  is close to one, thus leaving the radiation tail essentially unchanged. To be able to appreciate the improvement of this form with only three free fitting parameters against an often employed heuristic polynomial background fit, one must know that in our case the latter would require a polynomial of sixth to ninth order in  $E_f$  to fit the radiation tail function alone. Thus the heuristic polynomial fit is inadequate. If a low order polynomial were used, the radiation tail could not be fitted; a high order polynomial, however, would make the background selection arbitrary.

The line shape fitting procedure as such has been described in detail by Pitthan,<sup>16</sup> who also gives the reasons why one need not apply the radiative corrections to the giant resonance cross sections. All the resonances and clusters of states evaluated in this paper were found to be best described by a Breit-Wigner line shape for the  $B$ -value distribution (strength function)

$$\frac{dB}{dE_x} = \left| \frac{dB}{dE_x} \right|_{\max} \frac{(\frac{1}{2}\Gamma)^2}{(E_x - E_0)^2 + (\frac{1}{2}\Gamma)^2},$$

with  $E_x$  being the excitation energy,  $\Gamma$  = full width at half maximum and  $E_0$  the (excitation) energy of the maximum of the strength function.

There are some slight but important differences between the shape of the strength function and the cross section of the resonances which have been described by Pitthan<sup>16</sup> and more recently, in greater detail, by Gordon and Pitthan.<sup>17</sup> The resonance energies and widths given in this paper are those of the strength function and not those of the cross section, because the latter depends on primary energy and scattering angle, while the first does not. In accord with common practice, a best fit was determined when a minimum in chi-square  $\chi^2$  was found.  $\chi^2$  is defined as

$$\chi^2 = \sum^n (x_i - x_0)^2 / \sigma^2$$

( $x_i$  calculated value of cross section,  $x_0$  measured value of the cross section,  $\sigma$  standard deviation associated with  $x_i$ ). Related to this  $\chi^2$  distribution is the term degrees of freedom, defined as the number of experimental points (typically of the order 400, i.e., 10 per MeV) minus the number of parameters fitted (24, i.e., 3 for each of the 7 Breit-Wigner Lines used plus 3 for the background). The expected theoretical value for  $\chi^2$  (per degree of freedom) in our case is  $\chi_{\text{theory}}^2 = 1.00 \pm 0.08$ . Due to an interpolation process used to assemble the sum spectrum from the 10 counter ladder, our data points are not totally statistically independent and  $\chi^2$  is decreased by about 20%.

A resonance has to fulfill the following criteria before it is accepted in our evaluation. Its inclusion into the fit has to be necessary for a  $\chi^2 < 1$  and consistent values of position, width, and strength must be obtained for the several spectra taken at different momentum transfer.

Naturally there are other methods of evaluation possible. Instead of a line shape fit, Fukuda and Torizuka<sup>8</sup> have recently employed a model dependent so-called "multipole expansion" for re-evaluating their giant resonance data.<sup>5</sup> This method would correspond to fitting a four term Fourier series ( $E1$  to  $E4$ ) to five points (number of spectra taken). Further, it does away with one of the valuable advantages of ( $e, e'$ ), the possibility of a nearly model independent<sup>18</sup> analysis of ( $e, e'$ ) cross sections. Moreover, it also gives away one of the most beautiful features of giant resonances in medium heavy and heavy nuclei, namely the existence of coherent resonant states in the continuum. By the same token, with our method we will not be able to detect strength which is fairly evenly distributed over the continuum and does not show up

in resonant form as one may suspect for  $E4$  and higher multipoles, due to the many shell model states available to them.

### B. $B$ values and sum rules

The method of extracting  $B$  values from  $(e, e')$  in heavy nuclei where the Born approximation is no longer valid has been described most clearly by Ziegler and Peterson.<sup>18</sup>

In Born approximation the  $B$  value is defined for a nucleus with ground state spin  $0^+$  by the formula for the relative cross section:

$$\frac{\sigma}{\sigma_{\text{Mott}}} = \frac{4\pi}{Z^2} (2\lambda + 1) \left| \int j_\lambda(qr) \rho_{\text{tr}}(r) r^2 dr \right|^2$$

and the reduced transition probability

$$B(E\lambda) = (2\lambda + 1) \left| \int r^\lambda \rho_{\text{tr}}(r) r^2 dr \right|^2.$$

The second integral may be regarded as the first term of a power series development of the Bessel function under the first integral.

The cross sections (area  $A$  under the resonance) used in this paper were calculated from the fitting parameters by  $A = (\pi/2\Gamma \times \text{height})$ , i.e., they correspond to the resonance integrated from  $-\infty$  to  $+\infty$ .

Other units for transition strength beside the  $B$  values are ground state radiation width  $\Gamma_\gamma^0$  (eV), single particle units (spu), and percentages of sum rule strength. For the results of this work the following formulas were used:

$$\Gamma_\gamma^0 = \frac{8\pi\alpha}{[(2\lambda + 1)!]^2} \frac{\lambda + 1}{\lambda} \frac{E_x^{2\lambda+1}}{(\hbar c)^{2\lambda}} \frac{B(E\lambda)}{(2\lambda + 1)},$$

$$B(E\lambda)_{\text{spu}} = \frac{2\lambda + 1}{4\pi} \left( \frac{3R_0^\lambda}{\lambda + 3} \right)^2, \quad R_0 = 1.2A^{-1/3} \quad (\text{Ref. 19}),$$

$$S(E\lambda, \lambda > 1) = E_x B(E\lambda) = \frac{Z\lambda(2\lambda + 1)^2 \hbar^2}{8\pi M} \langle R^{2\lambda-2} \rangle_0 \quad (\text{Ref. 20}),$$

$$S(E1) = E_x B(E1) = \frac{9\hbar^2 NZ}{8\pi M A},$$

$$S(E0) = E_x |M_{fi}|^2 = \frac{\hbar^2}{M} A \langle R^2 \rangle_0 \quad (\text{Ref. 21})$$

( $\alpha = 1/137$ ,  $M_{fi}$  monopole matrix element,  $M$  proton mass).

Concerning the division of strength between isoscalar ( $\Delta T = 0$ ) and isovector ( $\Delta T = 1$ ) modes for  $\lambda = 0$  and  $\lambda > 1$  the usual assumption was made that a fraction  $Z/A$  goes into the isoscalar excitation and the remaining strength  $N/A$  goes into the isovector part. Since this division is based on the validity of the hydrodynamical model (surface oscillations), it poses only a problem for the mono-

pole excitation, where the role of the excess neutrons is unclear. The momenta  $\langle R^{2n} \rangle$  used in the sum rule calculation were determined by numerical integration of the ground state charge distribution as measured by  $(e, e)$ .<sup>13</sup> With the thus calculated  $\langle R^2 \rangle = 18.2 \text{ fm}^2$  and  $\langle R^4 \rangle = 452 \text{ fm}^4$ , the full energy-weighted sum rules (EWSR's) for  $^{89}\text{Y}$  have the values  $E_x B(E2) = 5.86 \times 10^4 \text{ MeV fm}^4$  and  $E_x B(E3) = 4.28 \times 10^6 \text{ MeV fm}^6$ .

## IV. RESULTS

### A. General

Figure 2 shows a spectrum of 92.5-MeV electrons scattered under  $105^\circ$  from  $^{89}\text{Y}$ . The spectrum has not been modified in any way, e.g., the dispersion correction has not been applied. The background drawn does not correspond to the real background; it is only intended to guide the eye. Several distinct features are apparent without a detailed analysis: (1) Lines with relatively small width at 2.5 and 4 MeV, (2) a doublet of lines at 7 and 8 MeV, (3) two wider resonances at 14 and 17 MeV, and (4) a very wide state at 28 MeV. Numerical analysis reveals that there are less strong resonances at 10.5 and 13.5 and possibly at 20 and 24 MeV. Since the one at 20 MeV was noticeable only at  $75^\circ$  and  $90^\circ$  where, according to Fig. 1, the  $E1$ , as compared with other multipolarities, is at a relative maximum, we concluded it to be the  $T_2$  part of the GDR. In contrast, the structure at 24 MeV shows up only at  $105^\circ$  and  $120^\circ$ . If taken to be real, it would be compatible with a strength of 20% of the isoscalar  $E3$  EWSR.

From the known systematics of the GR one would suspect that the resonances around  $14(63A^{-1/3})$ ,  $17(76A^{-1/3})$ , and  $28(125A^{-1/3})$  MeV are the  $E2$  ( $\Delta T = 0$ ),  $E1$  ( $\Delta T = 1$ ), and  $E2$  ( $\Delta T = 1$ ) GR, respectively. A look at Figs. 1 and 3 again verifies this idea: The change in peak height of the 14- and 17-MeV resonances between  $90^\circ$  and  $120^\circ$  as shown in Fig. 3 corresponds to the relative change in cross section as shown in Fig. 1.

All lines drawn in Figs. 3 and 4 had to be included in spectra from at least three angles to achieve a reasonable  $\chi^2$ . Omission of any one of them makes a consistent fit of all spectra and a  $\chi^2$  (per degree of freedom)  $\leq 1$  impossible.

### B. Giant dipole resonance and the breathing mode

The GDR, the prominent feature in photonuclear reactions, has been extensively measured in  $^{89}\text{Y}$  with quasimonochromatic photons.<sup>22,23</sup> From the  $(\gamma, n)$  cross sections one may, for a certain multipolarity, calculate the equivalent  $B$  value by the formula<sup>24</sup>

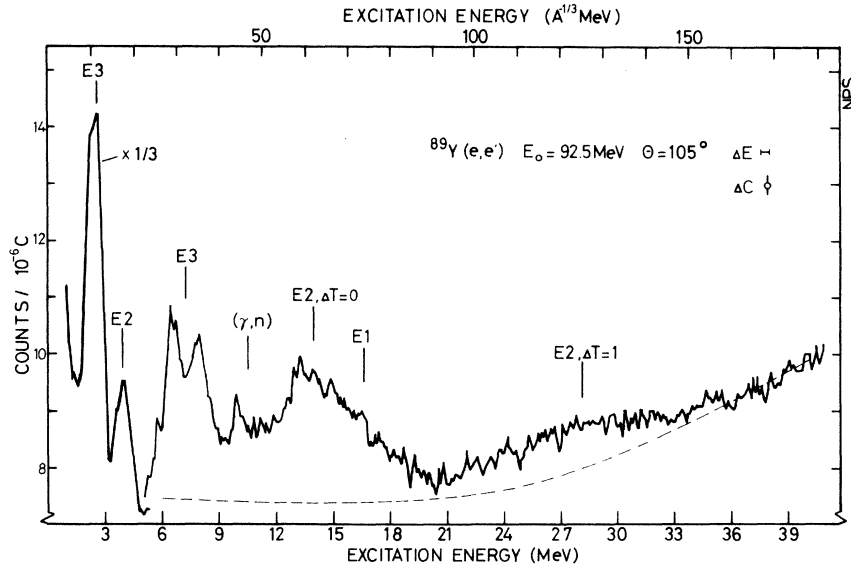


FIG. 2. Spectrum of 92.5-MeV electrons scattered inelastically at  $105^\circ$ . The background does not correspond to the real background, it is only intended to guide the eye. The count rate has not been corrected for the constant momentum dispersion of the magnetic spectrometer. Note the suppressed vertical scale. Excitation energy is given in units of  $A^{-1/3}$  MeV (upper scale) and MeV (lower scale).

$$\int \sigma_\gamma dE_\gamma = 8\pi^3 \hbar c \alpha \frac{\lambda + 1}{\lambda} \frac{1}{[(2\lambda + 1)!!!]^2} k^{2\lambda - 1} B(E\lambda, k)$$

with  $\alpha = 1/137$ ,  $\lambda$  multipolarity, and  $k = E_x/\hbar c$ .

The values thus calculated from  $(\gamma, n)$  are given

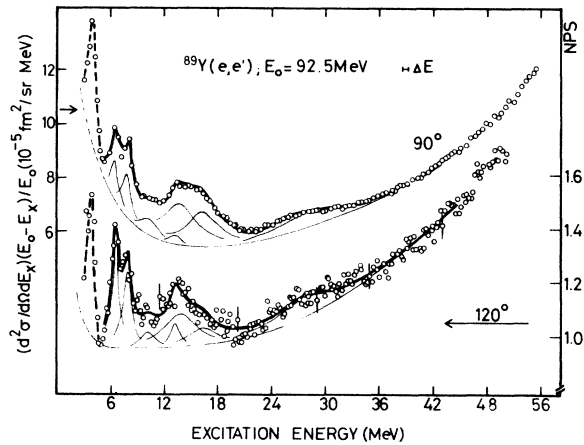


FIG. 3. Spectrum of 92.5-MeV electrons scattered inelastically from  $^{89}\text{Y}$  at  $90^\circ$  and  $120^\circ$ . Note that the scale for the  $90^\circ$  spectrum (left scale) is not suppressed. The resonances which were used for fitting the spectra and the background as described in the text are drawn. The spectra were taken and fitted with 10 data points per MeV. For graphical purposes the number of points for the  $90^\circ$  spectra was reduced in the continuum range by a factor of 4, the  $120^\circ$  spectra by a factor of 2. The fitting range was 5–45 MeV, the broken lines are drawn to guide the eye. The error for the  $90^\circ$  data is of the size of the data points.

in Table I together with other available results in  $N = 50$  nuclei. The results presented here were obtained by comparing DWBA cross sections,<sup>25</sup> calculated using the Tassie model,<sup>26</sup> [which leads to the same transition charge as the Goldhaber-Teller (GT)<sup>27</sup> model] with the experimental cross sections. Frequently the Steinwedel-Jensen<sup>28</sup> model is preferred for isovector resonances. However, the GT (Tassie) model with its simple dependence on the radius,

$$\rho_{\text{tr}}^{\text{GT}}(r) = C_{\text{GT}} r^{\lambda - 1} d\rho_0(r)/dr,$$

consistently describes the  $E1$  results in medium and heavy nuclei better than the GJ model and is therefore also used here. Figure 5 shows the Goldhaber-Teller DWBA cross sections compared with our results. We also have drawn the Steinwedel-Jensen cross section, calculated with the transition charge density

$$\rho_{\text{tr}}^{\text{SJ}}(r) = C_{\text{SJ}} r^\lambda d\rho_0(r)/dr$$

inserted into the DWBA program of Tuan *et al.* As apparent from Fig. 5, the Steinwedel-Jensen model, when fitted to the  $(e, e')$  data, fails to describe the cross section at the photon point (average from Refs. 22 and 23) by a factor of 2, while the Goldhaber-Teller model is in quite good agreement.

In our forward angle spectra we see a systematic deviation between 19- and 20-MeV excitation energy and in fact the insertion of a resonance improves the  $75^\circ$  and  $90^\circ$  fits. Figure 6 shows, with an extended scale, the region between 12 and 24

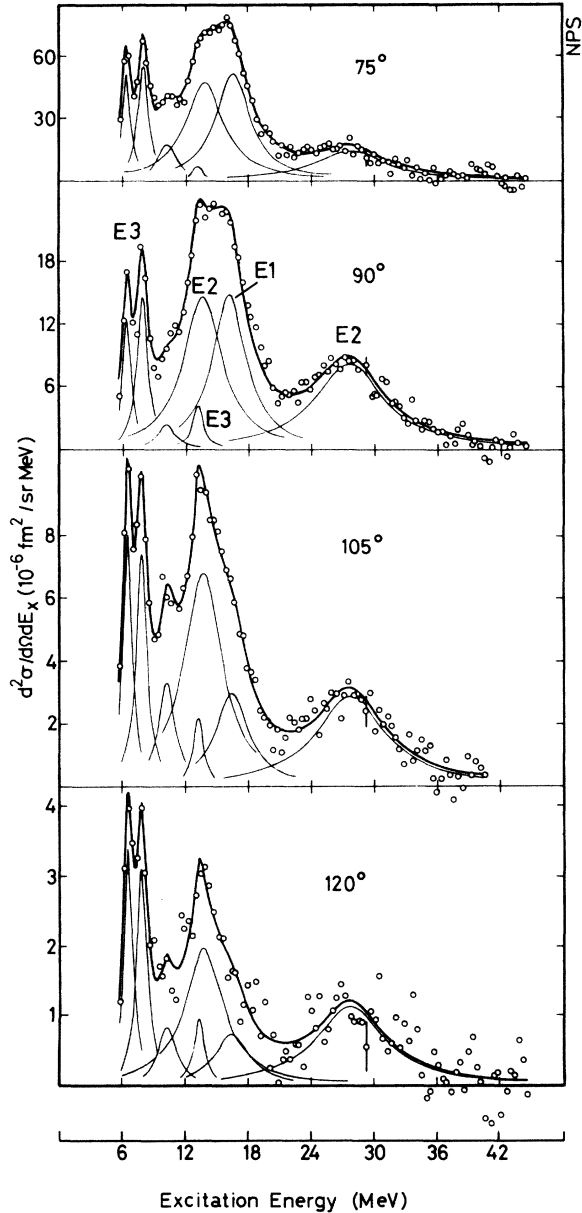


FIG. 4. 92.5-MeV electrons scattered inelastically from  $^{89}\text{Y}$  at  $75^\circ$ ,  $90^\circ$ ,  $105^\circ$ , and  $120^\circ$ . The fitted background (consisting of radiation tail, "target-in," and "target-out" background) as described in the text has been subtracted. The relative change in peak height of the single resonances, used and needed to decompose the cross section into its components, indicates very clearly the various multipoles contributing. Note that the cross sections fall off more than an order of magnitude between  $75^\circ$  and  $120^\circ$ . Apparent differences in comparison to Fig. 2, 3, and 7 are due to correction for the constant dispersion of the magnetic spectrometer which has been applied in this figure but not in the others and to the subtraction of the ghost peak around 7.5 MeV.

MeV at an angle of  $90^\circ$ , which shows both structures. As mentioned above, we identified the structure at  $\sim 20$  MeV with the  $T_2$  part of the GDR.<sup>29</sup> If we do so, we find  $(8 \pm 3)\%$  of the  $E1$  sum rule, in reasonable agreement with the value found in  $^{90}\text{Zr}$ .<sup>30</sup> To summarize the results for the  $E1$  resonance, we finally note that the  $T_2$   $E1$  strength found exhausts all of the strength predicted by  $(\gamma, n)$  measurements and dipole sum rule and that the strength and momentum transfer dependence is well described by the Goldhaber-Teller model.

These results are important in judging the merits of two proposals<sup>8,9</sup> which put the monopole breathing mode at 17 MeV in  $^{90}\text{Zr}$ . While  $^{89}\text{Y}$  is in principle a different nucleus and the resonances might be totally different in the two nuclei, in practice this seems to be highly improbable. Furthermore, the similarity of the electric giant resonances for neighboring nuclei has been demonstrated for La, Ce, and Pr.<sup>2,16</sup> In order to shed some light on this important problem we have calculated the  $(e, e')$  cross sections corresponding to 100% EWSR ( $E0$ ,  $\Delta T=0$ ) for an  $E0$  resonance at 17 MeV with a width of 4 MeV as proposed recently for  $^{90}\text{Zr}$ .<sup>8</sup> The result is drawn with a broken line into Fig. 7. It is important to note that we used the monopole program of the Sendai group<sup>31</sup> for the calculation. It is evident from this figure that there is not enough cross section to accommodate 100% EWSR. From our fits we may set an upper limit of 10%  $E0$  EWSR at 17 MeV. Thus, even the existence of a resonance with approximately 20% EWSR ( $E0$ ,  $\Delta T=0$ ) at 17 MeV as proposed by Marty *et al.*<sup>9</sup> for  $^{90}\text{Zr}$  seems not very likely. Finally, we would like to mention that the disagreement gets worse, if one uses the Steinwedel-Jensen model for the  $E1$  as in Ref. 8.

### C. Isoscalar giant quadrupole resonance

The observation of strong broad resonances in  $(e, e')$ <sup>2,32</sup> at an excitation energy of  $63A^{-1/3}$  MeV just below the GDR has brought about a renewed interest in the general properties in the nuclear continuum. A multitude of experiments has produced a wealth of information.<sup>33</sup> The overall features of position and strength of the GQR in nuclei with  $A > 40$  are well understood from both macroscopic<sup>34</sup> and microscopic<sup>35</sup> theories. Discrepancies between strength observed with various experimental methods for nuclei with  $A < 40$  seem to be understood.<sup>36</sup> The reason why we studied  $N = 50$  nuclei is the difference in width between  $E2$  and  $E1$  resonances of  $^{90}\text{Zr}$  (Ref. 5) compared with  $^{140}\text{Ce}$  (Ref. 16) or  $^{208}\text{Pb}$ .<sup>3</sup> There are no microscopic theories which correctly explain the width of giant resonances. A macroscopic approach us-

TABLE I. Comparison of some results for the  $E1$  (GDR) resonance in  $N=50$  nuclei.

Ref.	$E_0$ (MeV)	$\Gamma$ (MeV)	$R$ (%) <sup>a</sup>	Method	Nucleus
22	16.79	$3.95 \pm 0.06$	$87 \pm 6$	$(\gamma, n)$	$^{89}\text{Y}$
23	16.74	$4.1 \pm 0.1$	$111 \pm 5$	$(\gamma, n)$	$^{89}\text{Y}$
5	16.65	4.0	$107 \pm 32$	$(e, e')$	$^{90}\text{Zr}$
8	... <sup>b</sup>	4.0	$113 \pm 25$	$(e, e')$	$^{90}\text{Zr}$
This work	16.6	$3.9 \pm 0.2$	$104 \pm 10$	$(e, e')$	$^{89}\text{Y}$

$$^a R = E_x B(E1) / \text{EWSR}(E1, \Delta T = 1) \times 100.$$

<sup>b</sup>The authors used the  $(\gamma, n)$  value.

ing the concept of viscosity and the hydrodynamic model shows an overall agreement with the trend of the data as a function of nuclear mass, but does not account for shell effects.<sup>37</sup> Calculations for the effect of a deformed potential on the five sublevels of an  $E2$  state<sup>38</sup> describe the broadening in the deformed nucleus  $^{165}\text{Ho}$  (Ref. 39) quantitatively. Figure 8 shows that the resonance we find at 14.0 MeV with a width of  $(4.5 \pm 0.4)$  MeV follows an  $E2$  DWBA cross section. Compared with other experiments, Table II shows that only the excitation energies are in reasonable agreement in all of them. The most pronounced discrepancy is with the scattering of 155-MeV protons.<sup>40</sup> However, a systematic com-

parison with other available data shows that in all nuclei investigated, the half width and the strength of the  $E2$  state from Ref. 40 is smaller than results from other experiments.

The width from  $(\alpha, \alpha')$  scattering<sup>41</sup> is smaller than the width we find. It has been pointed out<sup>42</sup> that because the  $\alpha$  particle is relatively slow, the decay time of the resonance and the travel time of the  $\alpha$  in the nucleus are of the same order of magnitude. Rearrangement of the nucleons during that time could therefore influence the observed width. This speculation is backed by the observation<sup>6</sup> that  $\alpha$  data are generally better fitted by a Gaussian shape than by a Lorentz or a Breit-Wigner form, while the opposite is true for electromagnetic excitation.<sup>17</sup> Such effects should, however, not greatly influence the strength, and here our results are in excellent agreement with other experiments, except for the multipole expansion results.<sup>8</sup>

We conclude, therefore, that indeed the width of the isoscalar  $E2$  state at  $63A^{-1/3}$  MeV is greater than the width of the higher lying  $E1$  resonance, thus differing from results for heavier nuclei but in agreement with the viscosity model.<sup>37</sup>

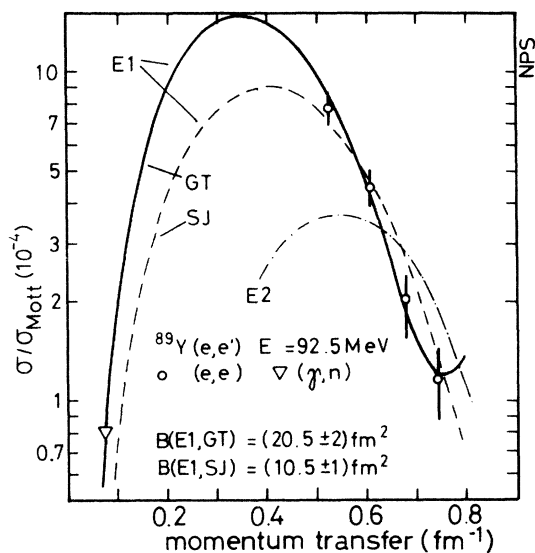


FIG. 5. Comparison of relative DWBA and experimental cross sections for the resonance found at 16.6 MeV. The Goldhaber-Teller model fits both the results of this work and the photon point from Refs. 22 and 23, while the Steinwedel-Jensen model, if fitted to the  $(e, e')$  data, misses the photon point by a factor of 2. An  $E2$  (or  $E0$ ) assignment of the cross section at 17 MeV can clearly be ruled out; as upper limit 5% of the isoscalar  $E2$  sum rule (or 10% of the isoscalar  $E0$  sum rule) may be estimated.

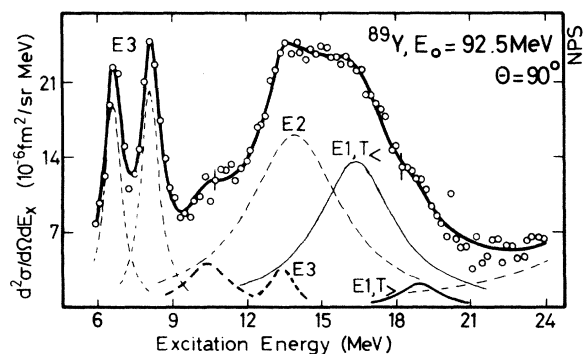


FIG. 6. Spectrum of 92.5-MeV electrons scattered inelastically at  $90^\circ$  from  $^{89}\text{Y}$ . The  $T > E1$  state is more clearly visible with this extended scale than in the  $90^\circ$  data of Fig. 3 or 4. The cross sections have been corrected for the constant momentum dispersion of the spectrometer.



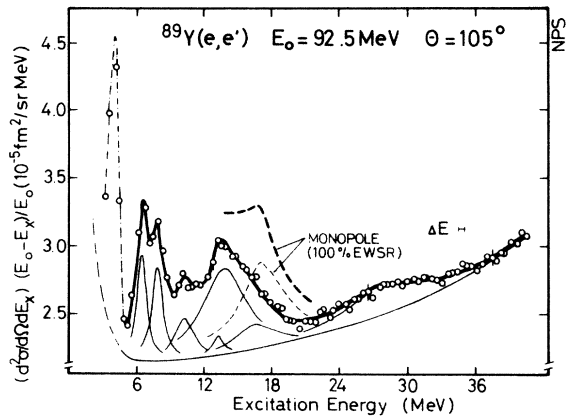


FIG. 7. Similar to Fig. 3, but for  $105^\circ$  and a fitting range of 5–40 MeV. The data are those of Fig. 2. The broken lines at 17 MeV indicate the height 100% of the monopole sum rule, as proposed by Ref. 8, would have in a resonance 4 MeV wide and how the composite cross sections would look.

#### D. Isovector giant quadrupole resonance

In contrast to the  $63A^{-1/3}$  state, the  $E2$  resonance predicted<sup>34</sup> and found<sup>4</sup> around  $130A^{-1/3}$  MeV is much less well known. The importance of both states for our understanding of nuclear dynamics has recently been emphasized.<sup>32</sup> In particular, it is important to know position, total width, and strength of both isoscalar and isovector parts of the quadrupole excitation to be able to fully test nuclear models.<sup>7</sup> Isovector resonances are only weakly (protons) or not at all ( $\alpha$  particle) excited by hadronic scattering. The  $\Delta T = 1$  resonances are therefore mainly open to investigation by radiative capture and electron scattering. While  $(e, e')$  does not measure isospin directly, the identification of the  $130A^{-1/3}$  resonance as the isovector  $E2$  state is aided by theoretical arguments.<sup>1</sup> The absence of this state in  $(\alpha, \alpha')$  is indirect experimental proof that this resonance is indeed isovector in nature.<sup>6</sup>

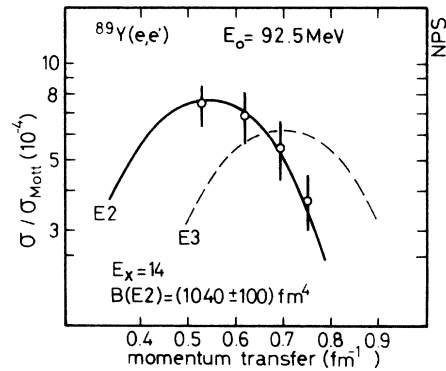


FIG. 8. Relative DWBA cross section, calculated using the Goldhaber-Teller model, as fitted to the experimental cross sections for the resonance at 14 MeV with a width of  $\Gamma = 4.5$  MeV. The comparison rules out any assignment other than  $E2$ .

The information available for this state has been collected by Paul.<sup>7</sup> While he found that the basic characteristics are already in evidence and that it will be difficult to learn more about this mode, Hanna<sup>33</sup> more recently emphasized the need for more detailed  $(e, e')$  experiments to establish the existence and universal nature of the isovector  $E2$  resonance as a coherent state.

The  $E2$ ,  $\Delta T = 1$  strength is found to exhaust approximately the full sum rule in heavy nuclei and is concentrated in a relatively small energy range (approximately 5 MeV).<sup>3</sup> It is split in deformed nuclei<sup>39</sup> and becomes wider for light nuclei.<sup>5</sup> Depending on the evaluation method employed, its strength seems to vary between 23%<sup>5</sup> and 73%<sup>8</sup> of the EWSR in the  $N = 50$  nucleus  $^{90}\text{Zr}$ . A recent proton capture experiment using the  $^{89}\text{Y}(p, \gamma_0)^{90}\text{Zr}$  reaction finds indication for  $E2$  (and  $E3$ ) strength above the GDR on the basis of a direct-semidirect model.<sup>43</sup> When the authors used the parameters from Ref. 8 for an  $E2$  ( $\Delta T = 1$ ) state at 26 MeV, the agreement between calculations and experiment improved, even though no structure of the cross

TABLE II. Compilation of some results for the  $E2$  ( $\Delta T = 0$ ) resonance in  $N = 50$  nuclei.

Ref.	$E_0$ (MeV)	$\Gamma$ (MeV)	$R$ (%) <sup>a</sup>	Method	Nucleus
5	14	$4.8 \pm 0.6$	$56 \pm 17$	$(e, e')$	$^{90}\text{Zr}$
6	$14.5 \pm 0.3$	$4.0 \pm 0.2$	$54 \pm 15$	$(\alpha, \alpha')$	$^{90}\text{Zr}$
8	$14^b$	$4.5^b$	84	$(e, e')$	$^{90}\text{Zr}$
40	$13.8 \pm 0.2$	3.2	$24 \pm 5$	$(p, p')$	$^{89}\text{Y}$
This work	$14.0 \pm 0.2$	$4.5 \pm 0.4$	$56 \pm 6^c$	$(e, e')$	$^{89}\text{Y}$

<sup>a</sup> $R = E_x B(E2) / \text{EWSR}(\Delta T = 0, E2) \times 100$ .

<sup>b</sup>Values were taken from Ref. 41.

<sup>c</sup>The rms radius  $R = 4.27$  fm of Ref. 13 was used for calculating the sum rule yielding an EWSR ( $E2$ ,  $\Delta T = 0$ ) of  $25\,800$  MeV fm<sup>4</sup>.

TABLE III. Compilation of results for the  $E2$  ( $\Delta T=1$ ) resonance in some  $N=50$  nuclei.

Ref.	$E_0$ (MeV)	$\Gamma$ (MeV)	$R$ (%) <sup>a</sup>	Method	Nucleus
5	27	...	23	( $e, e'$ )	<sup>90</sup> Zr
8	26	7	73	( $e, e'$ )	<sup>90</sup> Zr
43		...	$\approx 40$ <sup>b</sup>	( $p, \gamma$ )	<sup>90</sup> Zr
This work	$28.0 \pm 0.5$	10	$82 \pm 10$	( $e, e'$ )	<sup>89</sup> Y
		8	$57 \pm 6$		
		7	$48 \pm 5$		

<sup>a</sup>  $R = E_x B(E2) / \text{EWSR}(\Delta T=1, E2) \times 100$ . The  $\Delta T=1$  sum rule is connected with that of Table II by a factor of  $N/Z$ .

<sup>b</sup> The value for the sum rule percentage depends on the coupling used for the model.

section was found at 26 MeV. However, depending on the coupling, the  $E2$  capture strength had to be reduced to 40% EWSR in order to be compatible with the data.<sup>43</sup>

In our spectra for <sup>89</sup>Y we find a coherent resonance at 28 MeV (Fig. 4). The width is difficult to extract accurately because this resonance is both high in energy and very broad. If we assume it to be 7 MeV, which is also the smallest value found to fit the data,  $(48 \pm 5)\%$  of the EWSR ( $E2$ ,  $\Delta T=0$ ) is concentrated in this state. This value changes to  $(57 \pm 6)\%$  EWSR for  $\Gamma=8$  MeV. The maximum width which is still compatible with a  $\chi^2 < 1$  is  $\Gamma=10$  MeV (Table III). As described in the next section, this difficulty may be connected with a very wide structure at 45 MeV. Comparison of DWBA and experimental cross section for  $\Gamma=8$  MeV in Fig. 9 demonstrates that this resonance is clearly of  $E2$  character. The strength from the proton capture experiment is consistent with ours if we assume  $\Gamma=7$  MeV to be the correct width. Comparison of the change in width from <sup>208</sup>Pb to

<sup>89</sup>Y then would be in agreement with one prediction of the viscosity model,<sup>37</sup> namely, that the isovector width will vary more slowly with  $A$  than the isoscalar width.

In summary, we believe our data to be the best available for medium heavy nuclei in statistical accuracy. They clearly show the existence of a coherent  $E2$  state at  $125A^{-1/3}$  MeV which carries at least  $\sim 45\%$  and possibly as much as 80% of the isovector sum rule.

#### E. $E3$ strength

It has long been recognized that the low-lying octupole states in nuclei comprise only a small fraction of the energy-weighted sum rule and that more strength should be expected at higher energies. In particular, the missing  $1\hbar\omega$  strength has been predicted to lie at 5–6 MeV ( $30A^{-1/3}$  MeV) in heavy nuclei.<sup>34</sup> Indeed, such states have been found by electron scattering more than a decade ago.<sup>44</sup> A description of isoscalar and isovector strength, based on the concepts of the Bohr-Mottelson self-consistent model, has been made, among others, by Hamamoto<sup>45</sup> and is given in Table IV. Since the shell model allows both  $1\hbar\omega$  and  $3\hbar\omega$  transitions for octupole excitations, the situation is more involved than in the case of quadrupole excitations for which only  $2\hbar\omega$  is available for transitions into high-lying states. The  $E3$  strength is therefore more widely distributed and more difficult to locate.

The resonance found at approximately  $195A^{-1/3}$  MeV in heavy nuclei (44 MeV in <sup>89</sup>Y)<sup>3,39</sup> has been recently determined to be the isovector  $3\hbar\omega$  state.<sup>46</sup> As incentive for more experiments we would like to mention that we find systematic deviations between our data and the fitted background around 45 MeV which can be explained by a resonance about 15 MeV wide, and which possibly is responsible for the somewhat inconclusive result concerning the width of the  $E2$  ( $\Delta T=1$ ) state, described in the preceding section. But since there

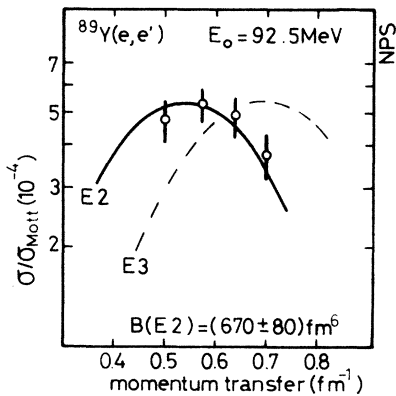


FIG. 9. Relative DWBA cross section using the Goldhaber-Teller model as compared with the resonance at 28 MeV assuming a width of  $\Gamma=8$  MeV. The comparison shows that the cross section in this region is predominantly  $E2$  with the possibility of some  $E3$  contribution.

TABLE IV. Shell model (random-phase approximation) predictions for excitation energy and strength of the  $E3$  transitions. The numbers were taken from Ref. 45 using  $\hbar\omega = 40A^{-1/3}$  MeV.

$E_x(\hbar\omega)$	Classic		$\Delta T=0$		$\Delta T=1$	
	$E_x (A^{-1/3} \text{ MeV})$	$R (\%)^a$	$E_x (A^{-1/3} \text{ MeV})$	$R (\%)^a$	$E_x (A^{-1/3} \text{ MeV})$	$R (\%)^a$
1	40	14	24	28	52	02
3	120	86	105	72	192	98

$$^a R = E_x B(E3) / \text{EWSR}(\Delta T, E3) \times 100.$$

is presently no way to prove that these difficulties are not based on deficiencies of our background procedure above 40 MeV, we are not yet able to quantitatively evaluate this region.

As mentioned earlier, the fits indicated a resonance between 19 and 20 MeV at forward, and 22 and 26 MeV at backward angles. The latter is consistent with a resonance carrying 20% EWSR ( $\Delta T=0$ ,  $E3$ ) and thus might be part of the ( $\Delta T=0$ )  $3\hbar\omega$   $E3$  state. It is noticeable, however, that the  $E2$  state at 28 MeV has a slight tendency to rise at backward angles relative to the DWBA cross section, thus possibly indicating nonresonant cross section of a high multipolarity.

We are able, however, to give more definitive results for the  $1\hbar\omega$  strength. At 13.5 MeV (Figs.

3, 4, and 6) we find an  $E3$  state of relatively small width ( $\Gamma = 1.2$  MeV) which carries  $(2.5 \pm 0.6)\%$  EWSR ( $E3$ ,  $\Delta T=1$ ). The comparison with DWBA calculations in Fig. 10 shows this state to be of  $E3$  character. Figure 1 shows that the only other assignment consistent with the angular distribution would be  $M2$ , which can be ruled out by strength arguments. Regarding the crudeness of Hama-moto's model,<sup>45</sup> the degree of agreement between her prediction of the strength and our result can only be called surprising, but it shows once more the conceptual correctness of the Bohr-Mottelson model.

Lower in energy, we find two groups of states centered at 6.75 and 8.05 MeV which also follow an  $E3$  form factor (Fig. 11) and carry 13% of the EWSR ( $E3$ ,  $\Delta T=0$ ). Together with the group of states at 2.6 MeV,<sup>13</sup> they exhaust all the expected  $1\hbar\omega$  ( $\Delta T=0$ ) strength (Table V). It should be specifically noted that their strength-weighted excitation energy of  $22A^{-1/3}$  MeV is in good agreement with the predictions.<sup>45</sup> The clusters at 7 and 8 MeV correspond to the well-known  $E3$  states at 5.4 MeV ( $\sim 32A^{-1/3}$  MeV) in  $^{208}\text{Pb}$  (Ref. 18) with 17% EWSR ( $E3$ ,  $\Delta T=0$ ). These types of states have recently been investigated more systematically

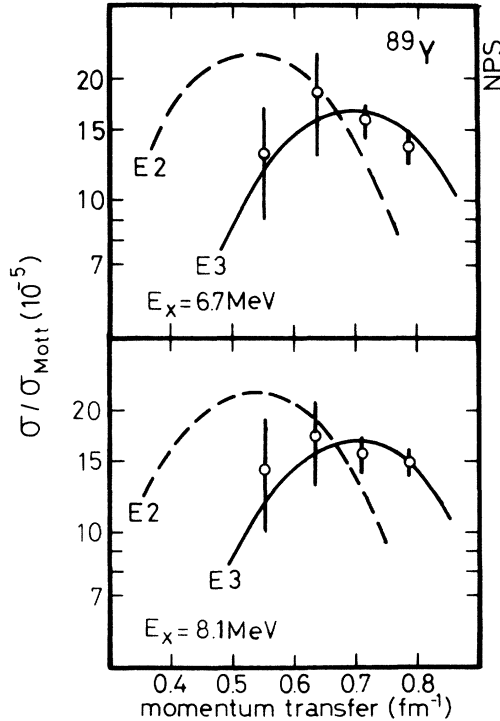


FIG. 10. Relative DWBA cross section using the Goldhaber-Teller model as compared with the cluster of states concentrated around 7 and 8 MeV. The comparison favors an  $E3$  assignment for these states. The large error at the lower momentum transfer is due to the subtraction of the ghost peak.

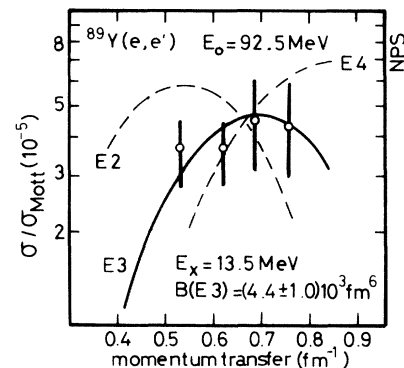


FIG. 11. Relative DWBA cross section calculated with the Goldhaber-Teller model for the structure at 13.5 MeV with a width of 1.2 MeV. Comparison with experiment favors an  $E3$  assignment.  $M2$  assignment would be possible, too, but was not considered seriously possible, due to the great  $M2$  strength necessary to explain the data.

TABLE V.  $1\hbar\omega$  E3 transitions in  $^{89}\text{Y}$ . The theoretical values were taken from Hamamoto (Ref. 45) and somewhat depend on the coupling used for the random-phase approximation calculations. One should note that the strength weighted energy for the  $\Delta T=0$  states is  $22A^{-1/3}$  MeV, close to the predicted value.  $R$  is defined in Table IV.

$E_x$ (MeV)	$\Delta T$	Experiment		Theory	
		$E_x$ ( $A^{-1/3}$ MeV)	$R$ (%)	$E_x$ ( $A^{-1/3}$ MeV)	$R$ (%)
2.6	0	12	$15.0 \pm 2.0$		
6.75	0	30	$5.5 \pm 1.0$	24	28
8.05	0	36	$6.5 \pm 1.0$		
13.5	1	60	$2.5 \pm 0.6$	52	2

with  $(\alpha, \alpha')$  in medium heavy nuclei.<sup>47</sup> There they were also found to cluster around  $32A^{-1/3}$  MeV as in  $^{208}\text{Pb}$  (Ref. 18) and the other  $(e, e')$  experiments<sup>44</sup> and were classified as the upper part of the  $1\hbar\omega$  isoscalar strength.

In summary, we have found all the expected  $1\hbar\omega$  E3 strength in  $^{89}\text{Y}$  (isoscalar and isovector) predicted by the shell model, but our data show only weak indication for  $3\hbar\omega$  states.

#### F. Other states

Our spectra show some other states which have been indicated in Figs. 2, 3, 4, and 6 but have not been discussed so far.

At 2.6 MeV we see a structure approximately 1 MeV wide. It has E3  $q$  dependence and is identical to three E3 states measured with higher resolution by Fivozinsky *et al.*<sup>13</sup>

Further up in energy a state at 4.0 MeV, not yet reported in the literature, is best described by an E2  $q$  dependence and carries a  $B(E2) = (700 \pm 100)$  fm<sup>4</sup>.

A state at 10.5 MeV could also be E2, but is better described by a mixture of M1 and E2. Since, however, we have restricted our measurements to forward angles, we cannot really disentangle E2 and M1. These backward angle measurements

would have to be carried out at an accelerator with higher incident current.

#### G. Errors

The errors given are the estimated total errors, which are larger than the statistical error would be. The estimate was based on how the areas under the curves changed during the fits due to different choice of resonance parameters, background, ghost peak subtraction, etc., while still maintaining  $\chi^2 < 1$ .

#### V. SUMMARY

We have measured the excitation range between 2 and 55 MeV in  $^{89}\text{Y}$ . Our general aim was to search for resonant structure in the continuum. Our data are in agreement with current ideas and macroscopic and microscopic calculations. For the quadrupole excitations of the continuum, we are able to cut down the error margin by a factor of 3. Our results are collected in Table VI.

The following points deserve special emphasis:

1. The isovector E2 strength is concentrated in a resonant state which comprises at least 45% of the isovector sum rule, if we use the minimum width compatible with the data (7 MeV), or as

TABLE VI. Compilation of all the results from this experiment.

$E_x$ (MeV)	$E_x$ ( $A^{-1/3}$ MeV)	$\Gamma$ (MeV) <sup>a</sup>	$B$ (fm <sup>2<math>\lambda</math>)</sup>	$R$ (%) <sup>b</sup>	$\Gamma_\gamma^0$ (eV)	spu	$\lambda$	$\Delta T$
2.6	...	$1.0 \pm 0.2$	$(1.12 \pm 0.15) \times 10^5$	$15 \pm 3$	$5.3 \times 10^{-6}$	34	3	0
4.0	...	$1.0 \pm 0.2$	$700 \pm 140$	$11 \pm 3$	$1.2 \times 10^{-1}$	6	2	0
6.75	30	$1.0 \pm 0.2$	$(16.5 \pm 3.0) \times 10^3$	$6 \pm 1$	$6.2 \times 10^{-4}$	5	3	0
8.05	36	$1.2 \pm 0.2$	$(16.5 \pm 2.5) \times 10^3$	$7 \pm 1$	$2.1 \times 10^{-3}$	5	3	0
13.5	60	$1.2 \pm 0.2$	$(4.4 \pm 1.0) \times 10^3$	$2.5 \pm 0.6$	$2.1 \times 10^{-2}$	1.4	3	1
14.0	63	$4.5 \pm 0.4$	$1040 \pm 100$	$56 \pm 6$	$9.0 \times 10^1$	8.8	2	0
16.6	74	$3.9 \pm 0.2$	$20.5 \pm 2.0$	$104 \pm 10$	$3.3 \times 10^4$	5.3	1	1
28.0	125	$\Gamma = 7$	$565 \pm 65$	$48 \pm 5$	$1.57 \times 10^3$	4.8		
		$\Gamma = 8$	$670 \pm 80$	$57 \pm 6$	$1.86 \times 10^3$	5.6	2	1
		$\Gamma = 10$	$960 \pm 130$	$82 \pm 10$	$2.67 \times 10^3$	8.1		

<sup>a</sup>The width may be either the width of the enveloping curve of unresolved discrete states or the width of a coherent resonant state.

<sup>b</sup> $R = E_x B(E\lambda) / \text{EWSR}(E\lambda, \Delta T) \times 100$ .

much as 80%, if we assume  $\Gamma = 10$  MeV to be correct. The problem of the width alone deserves further research.

2. We have found an  $E3$  state at 13.5 MeV which possibly can be identified with the  $E3$  ( $1\hbar\omega$ )  $\Delta T = 1$  excitation.

3. We do not see excess cross section in the region of the GDR which could accommodate the isoscalar monopole state in the strength recently proposed.

4. Together with the low-lying states at 1.6 and

3.1 MeV (3.5% EWSR) and 4.0 MeV [(11 ± 2)% EWSR], we find a total of 70% EWSR for the isoscalar  $E2$  strength in  $^{89}\text{Y}$ .

5. In contrast to our investigations of heavy nuclei, we do not see resonant  $3\hbar\omega$   $E3$  ( $\Delta T = 0$  or  $\Delta T = 1$ ) strength.

We would like to thank H. L. McFarland and D. D. Snyder for helping us keep the linac running and G. M. Bates and D. H. Dubois for their help in the long hours of collecting data.

† Work supported in part by the National Science Foundation and the Naval Postgraduate School Research Foundation.

\* Present address: at Varian Associates, Palo Alto, California 94303.

<sup>1</sup>A. Bohr and B. R. Mottelson, *Nuclear Structure* (Benjamin, Reading, Mass., 1975), Vol. 2, pp. 509, 639.

<sup>2</sup>R. Pitthan and Th. Walcher, *Phys. Lett.* **36B**, 563 (1971).

<sup>3</sup>R. Pitthan, F. R. Buskirk, E. B. Dally, J. N. Dyer, and X. K. Maruyama, *Phys. Rev. Lett.* **33**, 849 (1974); **34**, 848 (1975).

<sup>4</sup>R. Pitthan and Th. Walcher, *Z. Naturforsch.* **27a**, 1683 (1972).

<sup>5</sup>S. Fukuda and Y. Torizuka, *Phys. Rev. Lett.* **29**, 1109 (1972).

<sup>6</sup>D. H. Youngblood, J. M. Moss, C. M. Rozsa, J. D. Bronson, A. D. Bacher, and D. R. Brown, *Phys. Rev. C* **13**, 994 (1976).

<sup>7</sup>P. Paul, in *Proceedings of the International Symposium on Highly Excited States in Nuclei, Jülich, 1975*, edited by A. Faessler, C. Mayer-Böricke, and P. Türek, (KFA Jülich, 517 Jülich, W. Germany, 1975), Vol. 2.

<sup>8</sup>S. Fukuda and Y. Torizuka, *Phys. Lett.* **62B**, 146 (1976).

<sup>9</sup>N. Marty, M. Morlet, A. Willis, V. Comparat, and R. Frascaria, Université Paris-Sud, Institut de Physique Nucleaire, Report Orsay-PhN-76-03 (unpublished).

<sup>10</sup>K. L. Brown, *Advan. Part. Phys.* **1**, 71 (1967).

<sup>11</sup>C. R. Fischer and G. H. Rawitscher, *Phys. Rev.* **135B**, 377 (1964).

<sup>12</sup>H. A. Bentz, R. Engfer, and W. Bühring, *Nucl. Phys.* **A101**, 527 (1967).

<sup>13</sup>S. P. Fivozinsky, S. Penner, J. W. Lightbody, and D. Blum, *Phys. Rev. C* **9**, 1533 (1974).

<sup>14</sup>L. C. Maximon, *Rev. Mod. Phys.* **41**, 193 (1969).

<sup>15</sup>F. R. Buskirk and R. Pitthan, *Bull. Am. Phys. Soc.* **21**, 683 (1976) (unpublished).

<sup>16</sup>R. Pitthan, *Z. Phys.* **260**, 283 (1973).

<sup>17</sup>E. F. Gordon, M. S. thesis, Naval Postgraduate School, 1975 (unpublished); E. F. Gordon and R. Pitthan, *Nucl. Instrum. Methods* (to be published).

<sup>18</sup>J. F. Ziegler and G. A. Peterson, *Phys. Rev.* **165**, 1337 (1968).

<sup>19</sup>S. J. Skorka, J. Hertel, and T. W. Retz-Schmidt, *Nucl. Data* **A2**, 347 (1966).

<sup>20</sup>J. Weneser and E. K. Warburton, in *The Role of Isospin in Nuclear Physics*, edited by D. H. Wilkinson (North-Holland, Amsterdam, 1969).

<sup>21</sup>R. A. Ferrell, *Phys. Rev.* **107**, 1631 (1957).

<sup>22</sup>B. L. Berman, J. T. Caldwell, R. R. Harvey, M. A. Kelly, R. L. Bramblett, and S. C. Fultz, *Phys. Rev.* **162**, 1099 (1967).

<sup>23</sup>A. Leprêtre, H. Beil, R. Bergère, P. Carlos, A. Veyssièrre, and M. Sugawara, *Nucl. Phys.* **A175**, 609 (1971).

<sup>24</sup>D. B. Isabelle and G. R. Bishop, *Nucl. Phys.* **45**, 209 (1963).

<sup>25</sup>S. T. Tuan, L. E. Wright, and D. S. Onley, *Nucl. Instrum. Methods* **60**, 70 (1968).

<sup>26</sup>L. J. Tassie, *Aust. J. Phys.* **9**, 407 (1956).

<sup>27</sup>A. Migdal, *J. Phys. USSR* **8**, 331 (1944); M. Goldhaber and E. Teller, *Phys. Rev.* **74**, 1046 (1948).

<sup>28</sup>H. Steinwedel and H. Jensen, *Z. Naturforsch.* **5a**, 413 (1950).

<sup>29</sup>S. Fallieros and B. Goulard, *Nucl. Phys.* **A147**, 593 (1970).

<sup>30</sup>P. Paul, in *Proceedings of the International Conference on Photoneuclear Reactions and Applications, Asilomar, 1973*, edited by B. L. Berman (Lawrence Livermore Laboratory, Univ. of California, Livermore, 1973).

<sup>31</sup>Y. Kawazoe, *Res. Rep. Lab. Nucl. Sci. Tohoku Univ.* **6**, 211 (1973).

<sup>32</sup>B. R. Mottelson, *Science* **193**, 287 (1976); *Rev. Mod. Phys.* **48**, 375 (1976); and *Fysisk Tidsskrift* **74**, 97 (1976).

<sup>33</sup>S. S. Hanna, in *Proceedings of the International School on Electro- and Photoneuclear Reactions, Erice, 1976*, edited by S. Costa and C. Scharf, published in *Lecture Notes in Physics*, Vol. 61 (Springer, Berlin, 1977).

<sup>34</sup>B. R. Mottelson, in *Proceedings of the International Conference on Nuclear Structure, Kingston, 1960*, edited by D. A. Bromley and E. W. Vogt (Univ. of Toronto Press, Toronto/North-Holland, Amsterdam, 1960); A. Bohr, in *Nuclear Physics: An International Conference*, edited by R. Becker, C. Goodman, P. Stelson, and A. Zucker (Academic, New York, 1967).

<sup>35</sup>S. Krewald and J. Speth, *Phys. Lett.* **52B**, 295 (1974); I. N. Borzov and S. P. Kamerzhiev, *Yad. Fiz.* **21**, 31 (1975) [*Sov. J. Nucl. Phys.* **21**, 15 (1975)].

<sup>36</sup>A. Kiss, C. Mayer-Böricke, M. Rogge, P. Turek, and S. Wiktor, *Phys. Rev. Lett.* **37**, 1188 (1976).

<sup>37</sup>N. Auerbach and A. Yeverehyahu, *Ann. Phys. (N.Y.)* **95**, 35 (1975).

<sup>38</sup>N. Auerbach and A. Yeverehyahu, *Phys. Lett.* **62B**,

- 143 (1975).
- <sup>38</sup>G. L. Moore, F. R. Buskirk, E. B. Dally, J. N. Dyer, X. K. Maruyama and R. Pitthan, *Z. Naturforsch.* **31a**, 668 (1976).
- <sup>40</sup>N. Marty, M. Morlet, A. Willis, V. Comparat, and R. Frascaria, *Nucl. Phys.* **A238**, 93 (1975).
- <sup>41</sup>J. M. Moss, C. M. Rosza, J. D. Bronson, and D. H. Youngblood, *Phys. Lett.* **53B**, 51 (1974).
- <sup>42</sup>A. Schwierczinski, R. Frey, E. Spamer, H. Theissen, and Th. Walcher, *Phys. Lett.* **55B**, 171 (1974).
- <sup>43</sup>F. S. Dietrich, D. W. Heikkinen, K. A. Snover, and K. Ebisawa, *Phys. Rev. Lett.* **38**, 156 (1977).
- <sup>44</sup>H. Überall, *Electron Scattering from Complex Nuclei* (Academic, New York, 1971).
- <sup>45</sup>I. Hamamoto, in *Proceedings of the International Conference on Nuclear Structure Studies Using Electron Scattering and Photoreaction, Sendai, 1972*, edited by K. Shoda and H. Ui [Suppl. Res. Rep. Nucl. Sci., Tohoku Univ., **5**, 205 (1972)].
- <sup>46</sup>W. A. Houk, R. W. Moore, F. R. Buskirk, J. N. Dyer, and R. Pitthan, *Bull. Am. Phys. Soc.* **22**, 542 (1977).
- <sup>47</sup>J. M. Moss, D. H. Youngblood, C. M. Rosza, D. R. Brown, and J. D. Bronson, *Phys. Rev. Lett.* **37**, 816 (1976).